

FUNDAMENTAL STUDY OF NANOPOROUS NETWORK (NPN) CHARACTERISTICS ENABLING OUT OF AUTOCLAVE MANUFACTURING OF AEROSPACE-GRADE COMPOSITE LAMINATES

Alisa N. Webb¹, Jingyao Dai¹, Kwasi Asamoah-Addo², Justin Griffin², Stephen A. Steiner III², and Brian L. Wardle³

¹ Department of Aeronautics and Astronautics, Massachusetts Institute of Technology, Cambridge, MA, United States of America

² Aerogel Technologies LLC, Boston, MA, 02136, Web: www.aerogeltechnologies.com

³ Department of Aeronautics and Astronautics, Massachusetts Institute of Technology, Cambridge, MA, United States of America, wardle@mit.edu, Web: aeroastro.mit.edu/brian-wardle

Keywords: Nanoporous Networks, Porometry, Permeability, Capillary Pressure, Composites Manufacturing

ABSTRACT

Commonly-used autoclaves provide a source of convective heat and pressure to both cure and remove voids of aerospace-grade composites. However, such autoclave processing is energy intensive, suffers from size and throughput limitations, and has high infrastructure costs. By utilizing nanoporous networks (NPNs), a novel manufacturing technology, aerospace-grade composites can be produced with void free interlaminar regions with traditional oven curing techniques or Out-of-Oven (OoO) carbon nanotube (CNT) heaters. While aligned CNT forests were the first demonstrated NPN, it is of interest to study these and other common nanoporous materials for fundamental properties. Capillary flow porometry (CFP) directly measures capillary pressure and permeability, key characteristics of NPNs for composite manufacturing. X-ray microcomputed tomography (μ CT), and scanning electron microscopy (SEM) are used to characterize NPN structure. In this work, aerogel polymers, carbon nanotube (CNT) systems, Anodic Aluminum Oxide (AAO), and other common nanoporous polymers are investigated as candidates for NPN selection to be later applied to composite manufacturing of different composite polymer matrix systems.

1 INTRODUCTION

To produce void-free aerospace-grade composites with high fiber volume fractions, autoclaves provide environments of high pressure and temperature necessary to remove voids and to cure the composite laminates [1]. Voids weaken the structural properties of the composite and cracks that initiate from voids can cause reduction in the service life of composite parts [7]. In the autoclave, composites are put under vacuum while an external pressure, typically 7 bar, is applied to extract any trapped air bubbles and compress the laminas together [2]. As the temperature increases within the autoclave, resin flows throughout the composite layers causing each layer to become fully wet. However, due to the large energy and equipment costs associated with a temperature-controlled pressure vessel, along with the geometry constraints imposed by the autoclave's volume, more optimal manufacturing can be implemented [4]. This has led to the development of out-of-autoclave (OoA) systems that use convective thermal heat from an oven without the need for applied external pressure to manufacture aerospace-grade composites [3]. However, to minimize porosity of the composite, part size needs to be minimized, vacuum needs to be maintained for longer periods of time, and vacuum must have a larger differential pressure reading [8]. These considerations in sum lead to manufacturing constraints and limitations.

To approach the concerns of efficiency, an alternative approach has been developed which utilizes the NPNs' characteristics, especially their high capillary pressure to aid resin infusion and void removal of interlaminar regions of autoclave-grade prepreg laminas. In this work, commercially available NPNs such as CNT films, polymer membranes, and AAO membranes were selected and applied at the ply-ply interfaces of the composite structure. In past work, flat panels produced by unidirectional laminas have successfully worked with polyimide films at the ply-ply regions. Within this study, a woven laminate is introduced to demonstrate the effects of NPNs on more complex composite interfaces.

2 METHODS

2.1 Capillary Flow Porometry

NPN characteristics including capillary pressure and permeability can be investigated using capillary flow porometry. Using a gas-liquid porometer (POROLUX™ 1000), circular membranes with diameters of 25mm were placed into a membrane holder to derive dry and wet curves of the tested NPN materials. For dry curves, an inert gas, N₂, is applied at increasing pressure differences on both sides of the membrane, where the corresponding flow rate through the membrane is recorded. For wet curves, a similar procedure is completed; however, the membrane is fully wetted by a nontoxic wetting liquid with known contact angle and surface tension values. In this set of experiments, the wetting liquid used is perfluoroether with a surface tension of 16.39±0.02 mN/m. Pressurized nitrogen gas is then applied until the membrane is fully dry and the wet curve aligns with the previously measured dry curve [6]. Only through pores are characterized using this process, as only full openings produce flow rate for measurements. Due to the porous structure of these membranes, capillary rise occurs as a result of the surface tension between the liquid and gas mediums during the wet curve analysis. The wetting liquid in the larger pores is displaced first by the nitrogen gas. This can be seen from using Young-Laplace equation (Equation 1),

$$P_c = \frac{2 * n * \sigma * \cos \theta}{r_m} \quad (1)$$

where n is a geometric coefficient due to imperfect cylindrical pores, σ is surface tension of the liquid, θ is the contact angle between the liquid and pore wall, and r_m is the capillary radius. Lower capillary pressures are created from larger pore radii. In this work, capillary pressure is determined at the mean flow pressure where the half-dry curve and wet curve intersect. The half-dry curve is the measured dry curve multiplied by a factor of 1/2, resulting in half the slope of the linear curve. In Figure 1, a visual of a porous membrane in the process of a wet curve analysis is shown to demonstrate the displacement of the wetting liquid from the applied pressurized gas.

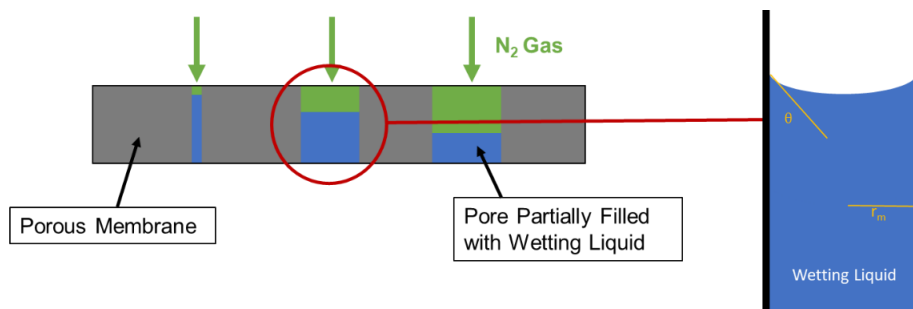


Figure 1: Capillary Flow Porometry on Non-Uniform Membrane

2.2 Scanning Electron Microscopy (SEM) Imaging and Microcomputed Tomography (μ CT)

SEM images were utilized to gain insight into the surface microstructure of the selected NPNs. Surface images obtained provided qualitative understanding into estimates of pore sizes, along with surface porosity. While capillary flow porometry is a useful tool in understanding the microstructure of a nanoporous architecture, it does not provide a full picture into the porosity of the material. X-ray μ CT (Zeiss Xradia Versa High-resolution 3D X-ray Imaging microscope) provides accurate thicknesses of the selected NPN membranes on a micro scale. The source of the device was set to a power of 7 Watts and 80 kilovolts without the use of a filter. The voxel size used for scanning ranged from 0.7 to 1.2 μm , resulting in an image resolution size that is three times larger. To demonstrate the void removal capability of NPNs, an 8-ply IM7/8852 woven laminate with a layup of $[0^\circ]_{4s}$ was fabricated with polymer aerogel NPNs placed at every ply-ply interface. Curing was conducted under vacuum on a hotplate using the manufacturer-recommended curing cycle. Post-cured composites were also examined by μ CT to check for void-free zones within the structure. Within this study, the woven laminate was scanned with a power of 6 Watts, 80 kilovolts, and a voxel size of 1.36 μm .

3 RESULTS AND DISCUSSION

The current selection of materials for this work includes porous hydrophilic polyvinylidene fluoride (PVDF) membrane, Celgard 2325, buckypaper (Tortech 358-H3A), AAO membrane, and polyimide (PI) aerogel films. The hydrophilic PVDF membrane is a single layer membrane of 128 μm nominal thickness. Celgard 2325 is a trilayer membrane of polypropylene/polyethylene/polypropylene with a nominal thickness of 29.1 μm . The Tortech CNT film is a membrane of randomly organized CNTs with an areal density of 7 g/m^2 and nominal thickness 20 μm . The AAO membrane is a ceramic structure of 120 nm pore size and nominal thickness 51.8 μm . Lastly, the aerogel films are supercritically dried polyimide aerogel films with nominal thicknesses of 69 μm (expected thickness 60 μm) and 151 μm (expected thickness 200 μm). The main selection criterion of these materials includes commercial availability. Other characteristics of consideration for these NPNs in composites manufacturing includes the NPN's melting temperature, conformability to the fiber laminas, and porosity.

During the layup process, NPNs are placed between composite laminas via a manual roller tool to ensure contact between the NPN and fiber lamina. The process is repeated $n-1$ times, where n is the number of prepreg plies within the produced composite. Once placed in the desired heating environment for curing, the pores within the NPN or radii of the NPN draw liquid up through capillary action. As the resin liquid flows through the NPN channel, it is transported and distributed between the two directly connected laminas; thus, causing continuous wetting of the direct composite laminas through the resin curing process. Along with desirable wetting properties, this capillary action caused by the NPN effectively distributes a pressure to the adjacent plies, analogous to the compressive pressure exerted in an autoclave environment. Other pressures within the composite curing system consist of resin pressure and gas pressure inside of the nanoporous network. In the traditional autoclave method, resin pressure and autoclave pressure overcome the gaseous void pressures within the laminas, while in the NPN system, the autoclave pressure can be replaced by the capillary pressure induced from the NPN assuming full conformability of NPNs at interlaminar interfaces. In autoclaves, a typical pressure of 7 bar is needed to achieve void-free interlaminar regions. For most NPN materials, the induced capillary pressure can exceed the 7 bar range, sufficient for void removal at interlaminar regions. The range of capillary pressure from each NPN is calculated through the first bubble point pressure, the pressure where the flow rate is considered no longer zero on the measured wet curve, and the smallest pore pressure, the pressure where the wet curve and dry curve intersect indicating full membrane dryness. In Figure 2, these ranges of potential capillary pressure are shown from the porometry results. Each pairing of colored lines represent a trial run of a dry and wet curve.

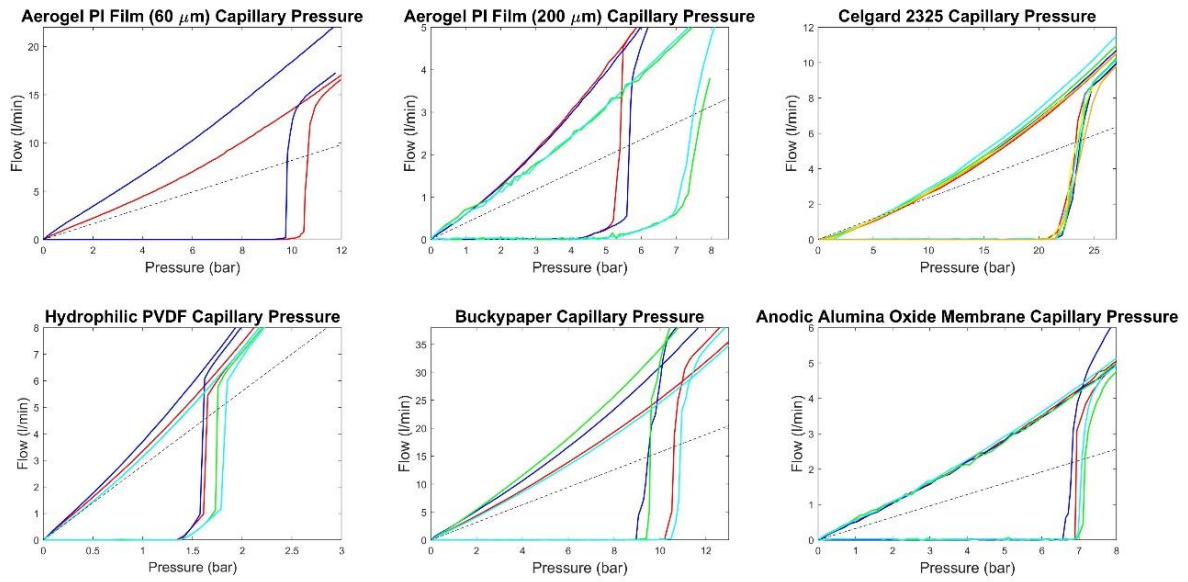


Figure 2: Capillary flow porometry results for each of the NPNs (Aerogel Films, Celgard, PVDF, CNT Film, and AAO Membranes). The half-dry curve's (dotted line) intersection with the NPN's curve demonstrates the material's capillary pressure value.

The lowest capillary pressure range is produced by the hydrophilic PVDF membrane, while the highest capillary pressure range is developed from the Celgard 2325 series. However, testing liquid flow and the epoxy resin flow behave differently throughout a nanoporous membrane due to varying surface tensions. The resin surface tension divided by the perfluoroether surface tension (16.39 ± 0.02 mN/m) is multiplied as a factor to the capillary pressure, while maintaining the contact angle of 0. The zero angle is maintained due to low surface tension energies in both the resin and testing liquid mediums. For woven laminates, it is proposed that continuous NPNs are selected to maintain pressure and conformability throughout the NPN and lamina interface.

Using the gas-liquid porometer, permeability was derived from the porometry dry curves via Darcy's Law (Equation 2).

$$Q = \frac{K * A * (p_i - p_o)}{(\mu * L)} \quad (2)$$

The variables are measured flow rate (Q), permeability (K), cross-sectional area (A), pressure difference between the inlet and outlet of the membrane ($p_i - p_o$), the porometer gas dynamic viscosity (μ), and NPN membrane thickness (L). Using the known area, known N_2 dynamic viscosity ($17.72 \mu\text{Pa}\cdot\text{s}$), and the measured flow rates and pressures, only the thickness of the membrane is unknown. Due to the microscale lengths of these NPNs, μCT was used to measure the through thickness of these membranes. Materials with high porosity were successful in the characterization regardless of the lower contrast between membrane and air. High aspect ratio tomography was used for the thin membranes to counteract the significant difference between thickness and width.

Utilizing capillary pressure and permeability results, infusion behavior was derived for an epoxy resin system flowing through a capillary or pore within NPNs. The flow of resin through the NPNs was modeled as a 1D Newtonian fluid flow due to the resin's low shear rate. Rearranging Darcy's Law, a flow front speed (Equation 3) is derived from the following equation:

$$\frac{dh_f}{dt} = \frac{K * \Delta P}{\varepsilon * \mu * h_f} \quad (3)$$

where h_f is the flow front position, ε is porosity, ΔP is the pressure gradient, and t is time. Integrating with respect to time results in an infusion speed to calculate the time taken for resin to fully wet the NPN layer. The full pressure gradient in this scenario is the resin pressure, atmospheric pressure, and capillary pressure induced by the NPN opposed by the gas pressure within the NPN. Due to the NPN being under vacuum, it is assumed that the gas pressure within the NPN is reduced to zero. Thus, capillary pressure and permeability are the key parameters to understanding NPNs as an enabler for vacuum-bag-only (VBO) composite manufacturing. Fig. 3 plots these key metrics for the different NPNs considered here. High permeability and capillary pressure are desirable to ensure void free interlaminar regions, likely leading to faster infusion times.

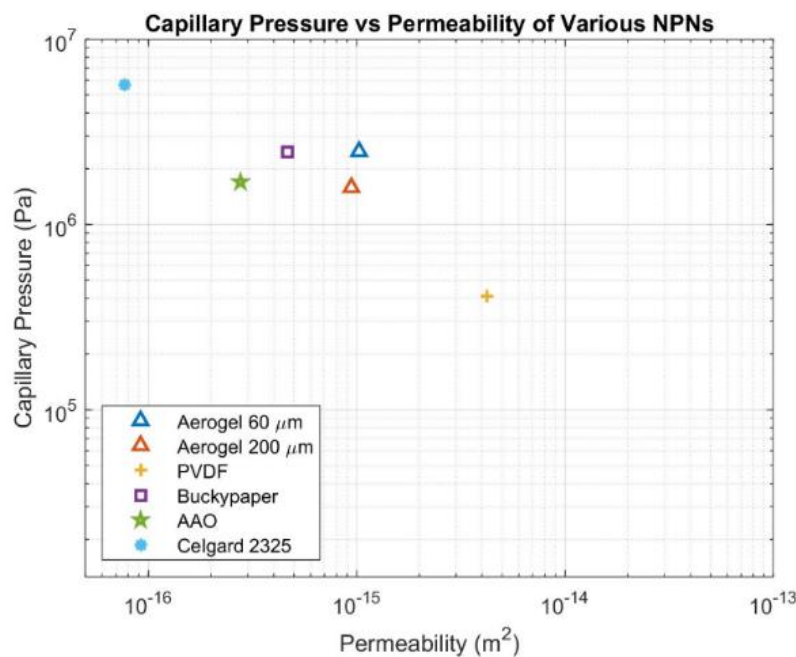


Figure 3: Logscale graph of capillary pressure versus permeability for each of the NPNs

As an example, an IM7/8552 woven composite laminate (HexPly® 8552) was cured using out-of-oven heating (vacuum-bag-only) into an 8-ply [0°]_{4S} panel as shown in Figure 4, using the 60 μm aerogel polyimide film at every ply-ply interface. To ensure the laminate and NPN system was a void-free composite, μCT was used to inspect throughout the volume. Previous baseline laminates without NPN application cured VBO had significant voids within the composite's microstructure at the interlaminar regions. Through inspection of the μCT scans, no voids are viewed at the interlaminar regions of the NPN-cured composite.

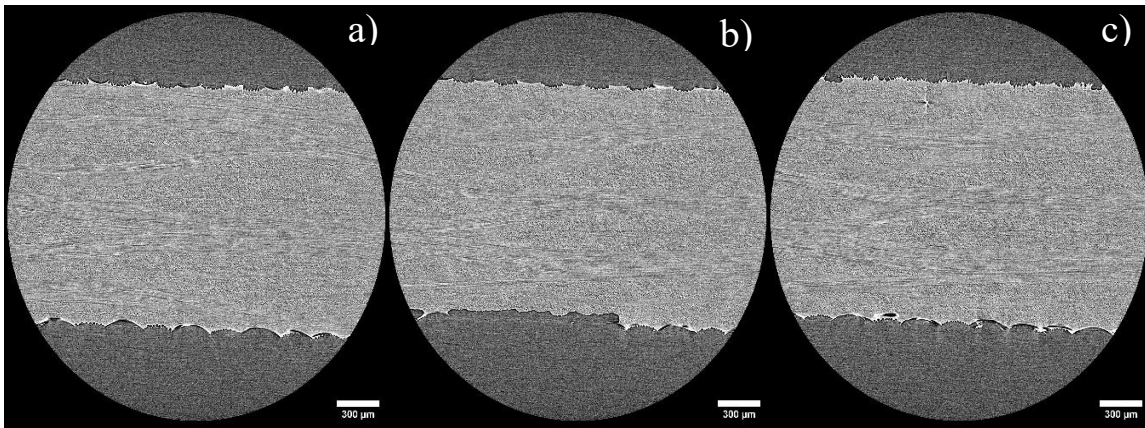


Figure 4: A series of three μ CT scans of an OoO-cured 8-ply $[0^\circ]_{4s}$ IM7/8552 composite at varying surface levels throughout the structure.

4 CONCLUSIONS

In summary, permeability and capillary pressure are characteristics dependent on the NPN's microstructure that provide insight into the infusion speed and void-free creation of aerospace-grade composites. NPNs were selected based on ease of access within industry. Then, these NPNs were individually tested for capillary pressure and permeability using capillary flow porometry and μ CT. Aerogel PI film 60 μ m, aerogel PI film 200 μ m, AAO membrane, Celgard 2325, and buckypaper all produced average capillary pressures above the 7 bar autoclave application. One dimensional infusion time modeling was derived for generalized use of any epoxy resin system compatible with the fiber lamina, pending temperature effects. The aerogel film of expected nominal thickness 60 μ m was implemented into a woven laminate to maintain void-free interlaminar regions exhibited by traditional composites autoclave manufacturing. In sum, the study provides a starting guide for NPNs to be used within various fiber and resin systems.

For future work, mechanical testing will be performed to explore mechanical properties including inter and intra-laminar shear strengths of the cured woven laminates. The infusion time framework will be characterized experimentally to explore the effect of a number of NPNs with varying microstructures within woven laminates. Additionally, an updated Ashby plot of NPNs will be created to provide a material selection guideline for this composite manufacturing technique.

ACKNOWLEDGEMENTS

This work in this paper is partially supported by the U.S Office of Naval Research (ONR) under grant/contract number N00014-20-1-2300, and partially supported by Airbus, ANSYS, Boeing, Embraer, Lockheed Martin, Saab AB, and Teijin Carbon America through MIT's Nano-Engineered Composite aerospace STructures (NECST) Consortium. For the first author, this material is based upon work supported by the National Science Foundation under Grant No. DGE-2141064. This material is based upon work supported in part by the U. S. Army Research Office through the Institute for Soldier Nanotechnologies at MIT, under Cooperative Agreement Number W911NF-18-2-0048. Micro-computed tomography instrumentation supported by the Office of Naval Research (ONR) under grant number ONR.N000141712068 through the Defense University Research Instrumentation Program (DURIP) is gratefully acknowledged. The authors gratefully acknowledge the members of necslab at MIT for technical support and advice, Professor Gregory Rutledge (MIT) and their group for use of their porometry equipment, and POROMETER for the capillary flow porometry results for Celgard 2325.

REFERENCES

- [1] D. Abliz, Y. Duan, L. Steuernagel, L. Xie, D. Li and G. Ziegmann, Curing Methods for Advanced Polymer Composites - A Review, *Polymers and Polymer Composites* Vol. 21, No. 6, 2013, pp. 341–348. (doi: 10.1177/096739111302100602)
- [2] T.J. Hank, J. Lee, S. Cassady, S. Kessler, S. Steiner and B.L. Wardle, Void-Free Vacuum-Bag-Only Composite Manufacturing with Autoclave-Grade Prepreg Using Capillary Effects of Polymer Electrospun Nanofibers and Aerogel Nanoporous Networks, *AIAA SCITECH 2022 Forum*, 2022 (doi: 10.2514/6.2022-1094)
- [3] J. Lee, X. Ni, F. Daso, X. Xiao, D. King, J.S. Gómez, T.B. Varela, S.S. Kessler, and B.L. Wardle, Advanced carbon fiber composite out-of-autoclave laminate manufacture via nanostructured out-of-oven conductive curing, *Composites Science and Technology*, 166, 2018, pp.150-159. (doi: 10.1016/j.compscitech.2018.02.031)
- [4] J. Lee, S.S. Kessler and B.L. Wardle, Void-Free Layered Polymeric Architectures via Capillary-Action of Nanoporous Films, *Advanced Materials Interfaces*, Vol. 7, No. 4, 2020, p. 1901427 (doi: 10.1002/ADMI.201901427)
- [5] J. Dai, A. Webb, J. Lee, L. Randaccio, J. Griffin, S.A. Steiner and B.L. Wardle, Out of Autoclave Manufacturing of Void-free Woven Aerospace-grade Carbon Fiber Reinforced Plastic Composite Laminates Using Capillary Effects of Aerogel Nanoporous Networks, *AIAA SCITECH 2023 Forum*, 2023 (doi: 10.2514/6.2023-0516)
- [6] A. Jena and K. Gupta, Advances in Pore Structure Evaluation by Porometry, *Chemical engineering & technology*. 2010, pp. 1241–1250 (doi: 10.1002/ceat.201000119)
- [7] S. Mazumdar, *Composites Manufacturing, Materials, Product, and Process Engineering*, CRC Press, Florida, 2001.
- [8] T. Centea, L.K. Grunenfelder, S.R. Nutt, A review of out-of-autoclave prepregs – Material properties, process phenomena, and manufacturing considerations, *Composites Part A: Applied Science and Manufacturing*, Volume 70, 2015, pp 132-154 (doi: 10.1016/j.compositesa.2014.09.029)
- [9] “HexPly 8552 MATERIAL PROPERTIES DATABASE for Use with COMPRO CCA and Raven.” 2009.